universe

IMPACT FACTOR 2.9

CITESCORE 3.6

Article

Falling into the Past: Geodesics in a Time Travel Metric

Colin MacLaurin, Fabio Costa and Timothy C. Ralph

Special Issue
The Physics of Time Travel

Edited by
Dr. Ana Alonso-Serrano, Prof. Dr. Matt Visser, Dr. Jessica Santiago and Dr. Sebastian Schuster

MDPI

https://doi.org/10.3390/universe10020095

universe

MDPI

Article

Falling into the Past: Geodesics in a Time Travel Metric

Colin MacLaurin [1], Fabio Costa [1,2] and Timothy C. Ralph [3,*]

[1] School of Mathematics and Physics, University of Queensland, Brisbane, QLD 4072, Australia; c.maclaurin@uq.edu.au (C.M.); fabio.costa@su.se (F.C.)
[2] Nordita, Stockholm University and KTH Royal Institute of Technology, Hannes Alfvéns väg 12, SE-106 91 Stockholm, Sweden
[3] Centre for Quantum Computation and Communication Technology, School of Mathematics and Physics, University of Queensland, Brisbane, QLD 4072, Australia
* Correspondence: ralph@physics.uq.edu.au

Abstract: We investigate timelike and null geodesics within the rotating "time machine" spacetime proposed by Ralph, T.C.; et al. *Phys. Rev. D* **2020**, *102*, 124013. This is a rotating analogue of Alcubierre's warp drive spacetime. We obtain geodesics that begin and end in the surrounding flat space region, yet achieve time travel relative to static observers there. This is a global property, as the geodesics remain locally future-pointing, as well as timelike or null.

Keywords: general relativity; closed timeline curves; time machines

Citation: MacLaurin, C.; Costa, F.; Ralph, T.C. Falling into the Past: Geodesics in a Time Travel Metric. *Universe* **2024**, *10*, 95. https://doi.org/10.3390/universe10020095

Academic Editors: Ana Alonso-Serrano, Matt Visser, Jessica Santiago and Sebastian Schuster

Received: 15 December 2023
Revised: 2 February 2024
Accepted: 10 February 2024
Published: 16 February 2024

1. Introduction

Exotic spacetimes including wormholes, warp drives, and time machines have been used to probe frontier physics concepts, despite being of physically dubious construction themselves. An early example is Gödel's [1] rotating universe which has a negative cosmological constant but motivated developments in relativistic causality [2]. More recently, the Kip Thorne group has studied billiard ball collisions in the context of wormhole spacetimes with closed timelike curves (CTCs) to see if a consistent mechanics may be determined from initial conditions [3,4]. Hawking argued that spacetimes of this type are unstable [5] as have others for different cases, including Krasnikov [6], but a more general argument has not emerged. Other authors have studied quantum particles in the presence of CTCs. Deutsch [7] described consistent evolutions using a quantum computation circuit model, which was clarified by Politzer [8] using a less abstract approach. An alternative approach to obtain consistent evolutions was described by Lloyd et al. [9] based on teleportation.

Closed timelike curves are spacetime trajectories that start and finish at the same spacetime event. Spacetimes that contain them may be referred to as time machine spacetimes, as they allow particles to travel into their own past. As well as in wormhole spacetimes, CTCs have have been found in rotating spacetimes, including rotating cylinders (studied by van Stockum), and the Kerr spacetime [10] that describes rotating black holes (albeit within an inner region that some consider unphysical). Tippett and Tsang [11] suggested a classification of time machine spacetimes into three classes. The first class is those that arise naturally in geometries with strong angular momentum. The Gödel and Kerr spacetimes previously mentioned are examples of this class. The second class is spacetimes designed specifically for time travel. These include metrics due to Ori and co-workers [12–14], the wormhole spacetimes discussed earlier, the spacetime of Mallary et al. [15], and Tippett and Tsang's spacetime [11]. The third class is spacetimes that are designed to produce superluminal travel but allow time travel as a natural consequence. The spacetime we investigate here is of this third type.

Alcubierre [16] proposed a "warp drive" spacetime with a localized bubble region which travels faster than light as determined by a distant observer. Other warp drive spacetimes that

have been proposed include those by Krasnikov [17], Olum [18], Natário [19] and Bobrick and Martire [20]. Everett [21] and Krasnikov [17] considered boosting between two different warp drive spacetimes and found that CTCs could be formed. Ralph and Chang [22] defined a "time machine" spacetime by incorporating an Alcubierre-like warp bubble, made to follow a circular loop, on a rotating platform. This allowed backwards-in-time travel for certain parameters and hence the explicit formation of CTCs by a relatively simple metric. The physical realizability of such a metric is uncertain due to the exotic matter required to produce it, which appears to be a generic feature of warp drive spacetimes [23]. However, its study may lead to useful advances in understanding.

In this paper, we study geodesics in the Ralph and Chang spacetime. Our main result is that, for a particular choice of parameters, we find timelike and null geodesics which transit the curved spacetime region and exit into flat space at an earlier time than when they enter, according to an observer in flat space. Timelike geodesics with this property have previously been identified by Fermi and Pizzocchero [24] for a different spacetime (belonging to class two), albeit one with a similar structure. Whilst the Ralph and Chang spacetime involves an Alcubierre "bubble" which travels around a circular path, here we will consider parameters for which the front of the bubble merges with the rear, forming a toric structure similar to [24]. Nevertheless, the metrics and their specific properties are distinct.

Our paper is arranged in the following way. In the next section, we describe the time machine metric, its derivation and how we parameterize it. In Section 3, we describe some properties of the time machine metric before outlining our method for finding certain classes of geodesics in Section 4. Section 5 describes our main results before we discuss and conclude in Section 6.

2. The Time Machine Spacetime

Conceptually, the Ralph and Chang time machine spacetime is a combination of Alcubierre spacetime, with a rotating disc in Minkowski spacetime.

2.1. Alcubierre Spacetime

Alcubierre [16] starts with coordinates (t, x, y, z) on a manifold, and a path $x_s(t)$ along the x-axis, where the "s" stands for spaceship. The goal was to choose a metric such that this path is timelike and geodesic. Alcubierre defined a region around the worldline, since called the "bubble", parametrized by a function f with value 1 on the worldline, and approximately 0 far from it. This f characterizes the amount of warp, and is discussed further in Section 2.4. $v_s(t) := dx_s/dt$ is the coordinate speed of the spaceship. Using the lapse–shift formalism (see [25], §21.4 for background), it suffices to use a shift 3-vector $\vec{b}^i = (-fv_s, 0, 0)$ and lapse $\alpha = 1$. Then, the Eulerian observers, meaning those orthogonal to the hypersurfaces $t =$ const but which we name "warp" observers, have 4-velocity $u^\mu_{\text{warp}} = (1, fv_s, 0, 0)$. They are geodesic since their 4-acceleration is a function of the lapse gradient [26], §4.3.3. For $f = 1$, they coincide with the spaceship worldline.

The coordinate speed v_s has no limits. However, we stress there is never faster-than-light motion locally, that is, a massive test particle's 4-velocity is never null nor spacelike. It has at most "'effective' superluminal travel" [27]. Furthermore, all valid 4-velocities are future-pointing, never past-pointing.

Alcubierre [16] briefly mentioned the case of an arbitrary lapse and shift. Here, the Eulerian observers are $u^\mu_{\text{warp}} = \alpha^{-1}(1, -b^1, -b^2, -b^3)$, with co-velocity ${}^{\text{warp}}u_\mu = (-\alpha, 0, 0, 0)$. We generalize this construction in Appendix C to allow observers with vorticity, which are not orthogonal to any hypersurface. In our approach, Alcubierre spacetime is obtained by starting with Minkowski spacetime, including the metric. Take the static observers $\mathbf{u} := \partial_t$ as a starting point, which is the coordinate basis vector $(1, 0, 0, 0)$ in some chosen inertial frame. Now, define a "warp shift" 4-vector field $\mathbf{b} := -fv_s\,\partial_x$, and "warp lapse" scalar $\alpha = 1$. These combine to add terms to the Minkowski metric, yielding the Alcubierre metric (Appendix C). Formally, our model is a single manifold with two Lorentzian metrics.

But physically, we interpret this as two separate spacetimes, or two separate regions ("time" periods) within a single spacetime.

2.2. The Rotating Disc

Use cylindrical coordinates (t, r, ϕ, z) on Minkowski spacetime. A disc rotating at constant (coordinate) rate $d\phi/dt =: \Omega \in \mathbb{R}$ has a 4-velocity field:

$$u^{\mu}_{\text{disc}} = (1, 0, \Omega, 0)/\sqrt{1 - \Omega^2 r^2}. \tag{1}$$

This is valid within the region $r < 1/|\Omega|$ for subluminal motion. Intuitively, this field describes material elements making up the disc; however, our focus is on abstract reference frames not materials science. The motion is Born-rigid, meaning its expansion tensor vanishes: $\boldsymbol{\Theta} = \mathbf{0}$. At any given point, the Lorentz factor relative to a "lab" observer ∂_t is $\gamma = -\langle \mathbf{u}_{\text{disc}}, \partial_t \rangle = (1 - \Omega^2 r^2)^{-1/2}$, where the angle brackets refer to the metric scalar product. The following vector field points in the tangent direction:

$$\xi^{\mu} = (\Omega r, 0, 1/r, 0)/\sqrt{1 - \Omega^2 r^2}. \tag{2}$$

It has unit length $\langle \boldsymbol{\xi}, \boldsymbol{\xi} \rangle = 1$ and is purely spatial according to the disc observers, meaning $\langle \mathbf{u}_{\text{disc}}, \boldsymbol{\xi} \rangle = 0$. Intuitively, these model little rulers, but technically they are merely vectors in an orthonormal pair.

2.3. Ralph and Chang Spacetime

The time machine spacetime family we consider was introduced and analyzed in Ralph and Chang [22]. Here, we give a novel derivation starting with Minkowski spacetime with the disc 4-velocity field, also called the "platform", $\mathbf{u} := \mathbf{u}_{\text{disc}}$. Next, add an Alcubierre-like warp shift in the tangential direction for each observer $\mathbf{b} := -f v_s \boldsymbol{\xi}$. Warp lapse $\alpha := 1$. $v_s \in \mathbb{R}$ is taken as a constant, and our specific choices of bubble functions f are given in the following section. The resulting metric is (Appendix C):

$$ds^2 = \frac{(f v_s + \Omega r)^2 - 1}{1 - \Omega^2 r^2} dt^2 - 2 \frac{f v_s r (1 + \Omega^2 r^2 + \Omega r f v_s)}{1 - \Omega^2 r^2} dt\, d\phi + dr^2 + \frac{r^2((1 + \Omega r f v_s)^2 - \Omega^2 r^2)}{1 - \Omega^2 r^2} d\phi^2 + dz^2. \tag{3}$$

This is Equation (5) in Ralph and Chang [22]. They call these the "lab" coordinates, because where $f = 0$, the metric reduces to $ds^2 = -dt^2 + dr^2 + r^2 d\phi^2 + dz^2$, which is locally Minkowski spacetime, and ∂_t reduces to the static "lab" observers. The value $r = 1/|\Omega|$ is not only a coordinate singularity but a curvature singularity for the spacetime parameters tested. This is the radius at which the spinning platform's tangential velocity is the speed of light. Hence, we enforce $f = 0$ in the region around $r = 1/|\Omega|$ throughout this paper, and as a result, Equation (3) reduces to the Minkowski metric there. Placing the point $r = 1/|\Omega|$ outside the region of curvature such that $f = 0$ in its vicinity is a sufficient condition for removing the singularity. An interesting question for future investigation would be to find necessary conditions such that the singularity is removed.

Note that t is not necessarily timelike. (This is determined by the hypersurfaces $t =$ const, which have normal covector dt, satisfying $\langle dt, dt \rangle = g^{tt}$, which may have any sign.) Similarly, the coordinate basis vector ∂_t is not necessarily timelike, and, likewise, ϕ and ∂_ϕ are not necessarily spacelike. On a partly related note, the standard lapse and shift quantities relative to the $t =$ const hypersurfaces differ from our "warp lapse" and "warp shift", even when t is timelike.

The metric of Equation (3) may be summarized as the following, for brevity:

$$g_{\mu\nu} = \begin{pmatrix} g_{tt} & 0 & g_{t\phi} & 0 \\ 0 & 1 & 0 & 0 \\ g_{t\phi} & 0 & g_{\phi\phi} & 0 \\ 0 & 0 & 0 & 1 \end{pmatrix}. \tag{4}$$

2.4. The Bubble Function f

The time machine spacetime was originally conceived as a warp bubble revolving about the origin [22]. If we write $\tilde{\Omega}$ for the bubble's (coordinate) rotation rate $d\phi/dt$, a constant independent of the platform rate Ω, then we might expect f to have the form:

$$f = f_{\text{rot}}(\phi - \tilde{\Omega}t) f_r(r) f_z(z), \tag{5}$$

where f_z is symmetric. However, in this paper, we drop the angular dependence for simplicity, leaving f rotationally symmetric. This can be thought of as the bubble reaching around the entire cylinder. Also, we do not give our f an explicit time dependence. Hence, it is a function of r alone, and in principle also of z. This describes a torus rather than a bubble.[1] Here, we use the bump functions in Figure 1, which vanish beyond a certain fixed r. The Gaussian-inspired function has the definition:

$$f(r) = \begin{cases} \exp\left(1 - \frac{1}{1-(r-2)^2}\right) & 1 < r < 3 \\ 0 & \text{otherwise,} \end{cases} \tag{6}$$

whereas the plateau function is:

$$f(r) = \begin{cases} \frac{1}{1+\exp\left(\frac{1}{r-1}+\frac{1}{r-2}\right)} & 1 < r < 2 \\ 1 & 2 \le r \le 3 \\ \frac{1}{1+\exp\left(-\frac{1}{r-3}-\frac{1}{r-4}\right)} & 3 < r < 4 \\ 0 & \text{otherwise.} \end{cases} \tag{7}$$

These are smooth but not analytic. We define the time machine region of spacetime by $f \neq 0$, which coincides with the curved region.

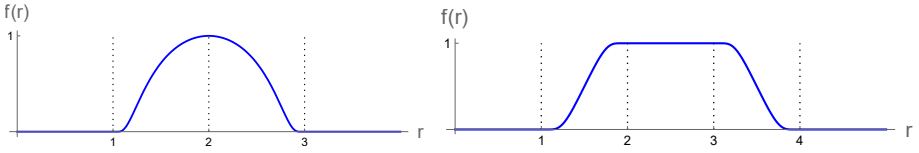

(**a**) (**b**)

Figure 1. Bump functions used for the bubble function f. The dotted lines indicate distinctive values of r. The choice of integer values is for simplicity, and also hints that f need not be finely tuned to achieve time travel. (**a**) A Gaussian curve squeezed into a finite domain. (**b**) A plateau function with ramps.

We can think of the z-dependence of f as being a broad plateau function centered on $z = 0$. However, we will start all our trajectories in the $z = 0$ plane, where they will remain, so the exact details of the z dependence will not play a role in our calculations. Similarly, the t dependence of f can be thought of as a broad plateau function centered on (but much broader than) the time interval of interest for the trajectories. In other words, we might envisage that at some time in the past, the value of f was slowly increased from $0 \to 1$. It then remained constant for an extended period, which includes the time of interest in this paper. At sometime in the future, it may be slowly decreased from $1 \to 0$, returning the

relevant spacetime to Minkowski. Hence, for the purposes of our calculations, f is taken to be constant in t and z.

3. Time Orientation and Warp Velocity

In Alcubierre spacetime, the Eulerian observers have co-velocity ${}^{\text{warp}}u_\mu = (-1,0,0,0)$. We observe that these are the same components as static observers in Minkowski spacetime, with whom our construction started. It turns out this is not a coincidence as shown in Appendix C. To obtain the analogous field in the time machine spacetime, first lower the index on the disc 4-velocity (Equation (1)) using the *Minkowski metric*, so ${}^{\text{disc}}u_\mu = (-1,0,\Omega r^2,0)/\sqrt{1-\Omega^2 r^2}$ in cylindrical coordinates, which is also ${}^{\text{warp}}u_\mu$. Now, raise the index using the *time machine metric*:

$$u^\mu_{\text{warp}} := \frac{1}{\sqrt{1-\Omega^2 r^2}}\left(1+\Omega r f v_s, 0, \Omega + \frac{f v_s}{r}, 0\right). \tag{8}$$

We denote this as the *warp velocity*. Equivalently, $\mathbf{u}_{\text{warp}} = \mathbf{u}_{\text{disc}} - \mathbf{b}$. It is unit timelike in the new metric: $\langle \mathbf{u}_{\text{warp}}, \mathbf{u}_{\text{warp}} \rangle = -1$. Where $f = 1$, it reduces to the bubble velocity defined in Ralph and Chang [22], though we have swapped the order of r and ϕ. Sharing the same co-velocity vector with the disc leads to interesting properties. For example, $\mathbf{u}_{\text{warp}}$ has the same Killing energy and angular momentum (defined in the following section) as the rotating disc frames do in Minkowski spacetime. One downside is that Equation (8) is only valid for $r < 1/|\Omega|$.

Another possibility is a local Lorentz boost of the warp observers by speed $\beta := \Omega r$ "backwards", which intuitively undoes the speed of the platform. Now, the vector $\boldsymbol{\xi}$ points in the tangential direction; while this is formally just the disc ruler vector from Equation (2), it also satisfies $\langle \boldsymbol{\xi}, \boldsymbol{\xi} \rangle = 1$ and $\langle \mathbf{u}_{\text{warp}}, \boldsymbol{\xi} \rangle = 0$ in the new metric. The local boost in the negative $\boldsymbol{\xi}$-direction is $\gamma(\mathbf{u}_{\text{warp}} - \beta\boldsymbol{\xi})$, or:

$$u^\mu_{\text{orient}} := \left(1 + \frac{\Omega r f v_s}{1-\Omega^2 r^2}, 0, \frac{f v_s}{r(1-\Omega^2 r^2)}, 0\right), \tag{9}$$

where $\langle \mathbf{u}_{orient}, \mathbf{u}_{orient} \rangle = -1$. This is an ideal *time orientation*, meaning a continuous timelike vector field. The expression remains valid for $r > 1/|\Omega|$, so we extend its range beyond the initial construction. In the flat space region $f \to 0$, it reduces to the lab observers ∂_t; hence, it agrees with the natural requirement that t increases towards the future in that region. It also agrees with the time orientation specified by the warp velocity on their region of overlap because they are related by a subluminal boost. A key point is that the time machine metric of Equation (3) is valid for $r < 1/|\Omega|$ and $r > 1/|\Omega|$, expanding the domain of applicability from what was considered in Ralph and Chang [22]. The metric retains a Lorentzian signature $-+++$ so it is a valid spacetime, despite not necessarily being constructed from a timelike platform. This is used in Section 5.2.

One may define the platform velocity as $u^\mu_{\text{plat}} := (1,0,\Omega,0)$ in the time machine spacetime (Appendix C). This may be timelike, null, or spacelike, and is not normalized as written. Similarly, for a revolving bubble, we may define the bubble velocity $u^\mu_{\text{bubble}} := (1,0,\tilde{\Omega},0)$, which is also un-normalized.

4. Method for Finding the Geodesics

4.1. Killing Vector Fields

It is natural to classify geodesics and other curves using Killing vector fields to whatever extent this is possible. For the general f in Equation (5), the bubble velocity $(1,0,\tilde{\Omega},0)$ is a Killing vector field. However, we drop the angular dependence, so the metric components are independent of t and ϕ. Hence, ∂_t is a Killing vector, and gives rise to an "energy" which is conserved along the geodesics:

$$e := -\langle \mathbf{u}, \partial_t \rangle. \tag{10}$$

Here, $\mathbf{u}$ is the tangent to a curve parametrized by proper time or proper length if non-null. Since ∂_t is not necessarily timelike, negative Killing energy is possible, but this is merely kinematics in contrast to the intrinsic negative energy of exotic matter. In addition, the Killing vector field ∂_ϕ defines a natural angular momentum ℓ which is conserved along the geodesics:

$$\ell := \langle \mathbf{u}, \partial_\phi \rangle. \tag{11}$$

Any trajectory with $z = 0$ everywhere is classified by e and ℓ at each point, along with the sign of the r component. Its tangent is expressed most simply with a lowered index:

$$u_\mu = \left(-e, \pm\sqrt{\epsilon + \frac{e^2 g_{\phi\phi} + 2e\ell g_{t\phi} + \ell^2 g_{tt}}{-g}}, \ell, 0 \right), \tag{12}$$

where $\epsilon := \langle \mathbf{u}, \mathbf{u} \rangle$ is $-1/0/1$ for a timelike/null/spacelike vector respectively, and $g := \det(g_{\mu\nu})$ evaluates to $-r^2$ for the time machine spacetime. However, this is only a "candidate" velocity, as it must satisfy several tests to be considered physical as follows.

4.2. Inequalities

We consider three tests of the tangent to a curve, ranging from essential down to desirable.

1. *Radicand test*. Equation (12) involves a square root, so the radicand must be non-negative. Otherwise, one's choice of e, ℓ and ϵ does not define a valid trajectory at that particular spacetime point. With the time machine metric components, this is:

$$\epsilon + e^2 - \frac{\ell^2}{r^2} + f v_s (\ell - e\Omega r^2) \frac{f v_s (\ell - e\Omega r^2) - 2r(e - \Omega\ell)}{r^2(1 - \Omega^2 r^2)} \geq 0. \tag{13}$$

2. *Future-pointing test*. Timelike and null tangents are required to be future-pointing if interpreted as physical particles. This is the local property: $\langle \mathbf{u}, \mathbf{u}_{\text{orient}} \rangle < 0$, which utilizes Equation (9), giving:

$$f v_s \frac{\ell - e\Omega r^2}{r(1 - \Omega^2 r^2)} - e < 0. \tag{14}$$

3. *Backwards-in-t test*. A desirable property of timelike and null tangents is to have $u^t < 0$ for at least part of the curve. We seek paths with time travel, in the sense of returning to a lab observer worldline at an earlier lab time. For lab observers, t is the proper time, and t must increase in the flat region. Note that we make no insinuation of global simultaneity but have merely used the continuity of t on the manifold. Now, $u^t < 0$ is:

$$e + f v_s \frac{\Omega r(e - \Omega\ell) + (e\Omega r^2 - \ell)(1 + \Omega r f v_s)/r}{1 - \Omega^2 r^2} < 0. \tag{15}$$

This trio of simultaneous inequalities is solvable as a large number of separate cases if we treat f as being independent of r as a first step. One may also show some simpler statements, for example, the restriction $r < 1/|\Omega|$ implies $\Omega v_s < 0$, so these parameters have opposite signs. In the flat region $f = 0$, timelike and null test particles must have positive energy, an increasing t coordinate, and $\epsilon + e^2 - \ell^2/r^2 \geq 0$.

4.3. Circular Paths

Circular trajectories are a simpler special case and aid in the discovery of other trajectories. With $r = \text{const}$ and $z = 0$, the candidate tangent is:

$$u_\mu = \left(\frac{\ell g_{t\phi} - \pm\sqrt{-g(\ell^2 - \epsilon g_{\phi\phi})}}{g_{\phi\phi}}, 0, \ell, 0 \right). \tag{16}$$

The '±' indicates there are two possible solutions for the circular trajectories. It can be shown to correspond to the sign of u^t, at least when the latter is nonzero. Hence, it must be -1 to pass the backwards-in-t test. Note that e and ℓ are not independent because of the constraint of circular motion; rather, $e = -u_t$ may be read off from Equation (12).[2] The radicand test is $\ell^2 \geq \epsilon g_{\phi\phi}$, and the future-pointing test is $\langle \mathbf{u}, \mathbf{u}_{\text{orient}} \rangle < 0$.

Again, these simultaneous inequalities are solvable, assuming that, at first, f is independent. For instance, in the case $\epsilon = -1$ and $r < 1/|\Omega|$, we must have either $\Omega r f v_s < -(1 + |\Omega| r)$; or else $-(r + 1/\Omega) < r f v_s < (r - 1/\Omega)$ together with:

$$\Omega \ell \geq |\Omega| r \sqrt{\frac{\Omega^2 r^2 - (1 + \Omega r f v_s)^2}{1 - \Omega^2 r^2}}. \tag{17}$$

Whilst for many cases now, requiring ℓ and e to be constant along a trajectory is necessary and sufficient to find the geodesics (such as the free-fall cases considered in the next section), this is not sufficient when circular motion is imposed. Given that ℓ and e are constant along a circular path, we further require that the particle feels no acceleration. The vector field $\mathbf{a} := \nabla_{\mathbf{u}} \mathbf{u}$, called the 4-acceleration for $\epsilon = -1$, is directed radially:

$$a^\mu = \left(0, \frac{\ell^2 (1 - r g'_{\phi\phi}/g_{\phi\phi}) \pm \ell \sqrt{\ell^2 + g_{\phi\phi}} (g'_{t\phi} - g_{t\phi} g'_{\phi\phi}/g_{\phi\phi}) + g_{\phi\phi} - \frac{1}{2} r g'_{\phi\phi}}{r g_{\phi\phi}}, 0, 0\right). \tag{18}$$

A dash means derivative with respect to r. We used the determinant of the metric $g = -r^2$. It is computationally simpler to obtain the co-acceleration using $\mathbf{a}^\flat = \mathbf{u} \lrcorner d\mathbf{u}^\flat$ (Appendix B). Now, $\mathbf{a} = \mathbf{0}$ for an affinely parametrized geodesic. This does not typically have an exact solution for r. But conversely, if the spacetime parameters and a specific value of r are substituted, then this rearranges to a quadratic in ℓ^2—that is, a quartic with terms in ℓ^4, ℓ^2, and 1. See Figure 2 for example solutions.

The abundance of circular geodesics suggests a strategy for time travel. Set up a test particle with ℓ and r chosen from the figure, and the corresponding e for circular motion, perhaps via a collision. It will accumulate negative t indefinitely, up to the time machine's construction, or aside from any orbital instabilities. Then, arrange a collision to bump the particle out. From a lab frame, this may mean orchestrating the exit collision before the test particle is sent in. A different strategy is to pick a trajectory which is not circular but has similar parameters to a those of a circular geodesics. Most of our examples will be like this, starting from the flat region, making several roughly circular loops in the curved region and then exiting.

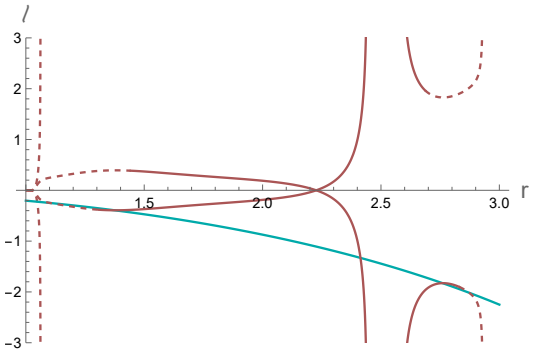

Figure 2. Timelike circular geodesics for $\Omega = -1/5$, $v_s = 7$, and the Gaussian-like f. The brown curves give the angular momentum required at each r. There are four candidate geodesics just above $r = 1$, and none near $r = 5/2$ nor just below $r = 3$. The dashed parts of the curves are not time-traveling: they are either past-pointing or have $u^t > 0$. The aqua curve is the warp velocity, included for comparison. The flat region(s) are not shown; there, the only constant–r geodesics have $\ell = 0$, the lab observers.

5. Free Fall to the Past

A very interesting situation is if particles can free fall from flat space into the time machine metric region and scatter back into flat space in such a way that they emerge in the past. We find such trajectories are possible given particular conditions for the metric and the initial trajectories. These trajectories do not form CTCs as such; indeed, closed loops are not what we desire for time travel. However, it is important to demonstrate in an operational way that there are events on the outward part of the trajectory that are indeed in the past of events on the inward part of the trajectory. We introduce a correction term that achieves this.

We start from the geodesic velocity field defined by Equation (12) for parameters where the physicality conditions, Equations (13) and (14), are satisfied. Then, for specific initial conditions (i.e., a particular incoming geodesic in flat space), the relevant geodesic in the region of curvature is calculated numerically from the velocity field. Timelike geodesics are found when $\epsilon = -1$ and null geodesics when $\epsilon = 0$.

5.1. Timelike Geodesic Examples

In this section, we present timelike time-traveling geodesics in the spacetime with parameters $\Omega = -1/5$, $v_s = 7$, and the Gaussian-like f of Equation (6). The case of circular geodesics for the same parameters was already considered in Figure 2; however, these are stuck inside the time machine. Figure 3 exhibits a geodesic that achieves time travel, while starting and ending in the flat region.

In Figure 3b, the exit (orange) curve typically has a lesser t-value than the entry (green) curve, within the region shown. The t–r plot has striking steepness at $r \approx 2.64$, which corresponds to the outer loop in Figure 3a. Here, the trajectory parameters are close to those of a circular geodesic at that point, including the e; this appears as a point near the lower-right in Figure 2.

One way to unambiguously achieve time travel is if the particle returns to a given lab location at an earlier lab time. Now, a lab worldline appears vertical in the spacetime diagram; however, most apparent intersections actually have angular separation in ϕ. In the flat region, it is natural to use t as a simultaneity convention, as this is a proper time for the lab observers and is Poincaré–Einstein synchronized, meaning $t = \text{const}$ is orthogonal to ∂_t. This justifies calling it an earlier lab time; however, this is largely just a convention. Physical or operational evidence would be the ability to send a causal signal from an outgoing event to an ingoing event. Suppose a lab observer is at some location along the ingoing curve. Time travel is achieved if there exists a timelike or null curve from the end (orange curve, later particle proper time) back to the start, arriving before the particle begins.

Suppose our causal signal is a null signal, sent along a circular arc at the time machine boundary, guided by an optical fiber, say. This curve segment takes lab time $\Delta t_{\text{arc}} = r|\Delta\phi|$, where the angular separation is at most π. Because we have not incorporated all possibilities, any conclusions that a given test particle trajectory achieves time travel should be understood as a sufficient condition but not necessary. Another approach is to compute the finite Minkowski interval between two points; this gives the length of a signal geodesic *if* the entire line passes through flat space. Another possibility is to send a geodesic signal though the curved region, but this calculation is more involved.

For the example trajectory, at $r = 3$, the t-difference is ≈ -6.5. Assuming our geometric units are meters, then 1 m of time is $1\ \text{m}/c \approx 3.3$ nanoseconds in SI units. The angular separation of $\approx 25^\circ$ (see Figure 3a) wastes ≈ 4.4 ns, but in total the signal arrives with $\Delta t \approx -17$ ns, which is before the particle leaves! For any readers creating their own plots, other time-traveling timelike geodesics with the Gaussian f include $\Omega = -1/5$, $v_s = 4.85$, $e = 1.9$, and $\ell = -2.08$; or $\Omega = -1/4$, $v_s = 5.5$, $e = 1.5$, and $\ell = -3.22$. These are adjusted so the ϕ-values roughly coincide at the boundary $r = 3$.

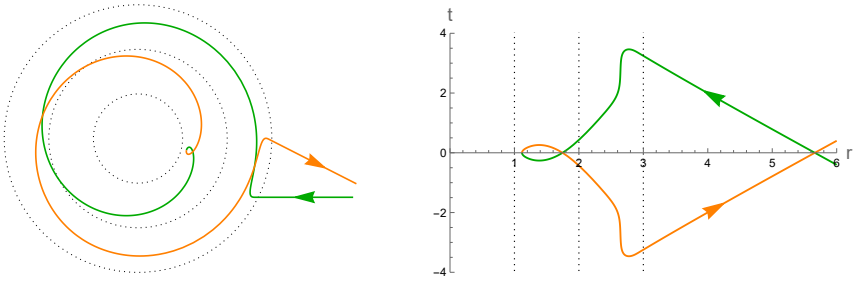

(**a**) (**b**)

Figure 3. Example timelike geodesic with $e = 2$, $\ell = -2.28$, and $z = 0$. The "space" diagram shows the test particle entering from the right, moving inwards along the green curve. The dotted lines mark significant values of f, as in Figure 1a, with the outermost one being the boundary of the time machine region. Soon after entering, the particle is swept around. Its exit path where r is increasing is colored orange. The "spacetime" diagram shows the same trajectory. In the flat space region, its t-coordinate must increase. But inside the time machine, its t-value mostly decreases, in this case. Yet, the trajectory remains future-pointing, i.e., the arrows on the trajectories indicate the direction of increasing proper time for the particle. It exits at an earlier t than it entered, but t must increase again thereafter. Still, a well-positioned lab observer would see the particle exit before it entered, so time travel is achieved. (**a**) "Space" diagram, the r–ϕ plane. (**b**) "Spacetime" diagram.

To summarize the situation depicted in Figure 3a, the region of curvature is a cylinder of outer radius 3 m and inner radius 1 m. The particle moves in the $z = 0$ plane. If the particle was to send a signal as it exits the region of curvature (orange curve, just outside the outer dotted radius), it would arrive at the entry point of the particle (green curve, just outside the outer dotted radius) approximately 17 nanoseconds before it enters.

5.2. Null Geodesic Examples

In this section, we consider null geodesics in the spacetime with parameters $\Omega = 1.2$, $v_s = 1$, and the plateau f from Equation (7). Hence, in this section, the region of curvature is a cylinder of outer radius 4 m and inner radius 1 m. Note that this means our time machine spacetime ($f \neq 0$) is in the region $r > 1/|\Omega|$ for this section. Figure 4 shows an example trajectory chosen for its significant time travel. At the time machine boundary $r = 4$, the difference between the t coordinates for the ingoing and outgoing path segments is -46 m to the nearest integer, or -152 ns. The angular difference here is 74°, which would take 17 ns for a causal signal to circumnavigate. The total time travel in our reckoning is still a respectable $\Delta t = -135$ ns.

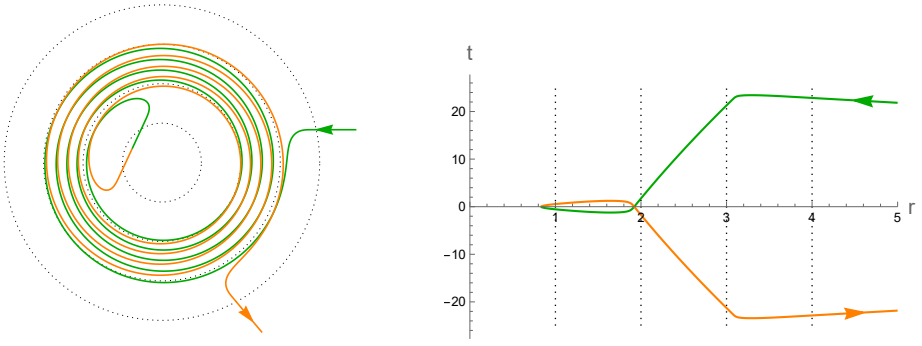

(**a**) (**b**)

Figure 4. Example null geodesic with $\ell/e = 0.8337$ and $z = 0$. As before, the dotted lines mark significant values of f, in this case from the plateau bump function as in Figure 1b. The test particle completes many loops at the plateau itself where $f = 1$, accruing a lot of negative t. Note the vertical axis scale on the spacetime diagram. (**a**) "Space" diagram, the r–ϕ plane. (**b**) "Spacetime" diagram.

We focus on null geodesics, which start from the flat region, and hence have positive energy: $e > 0$. Conveniently, their paths are classified by impact parameter ℓ/e, up to rotational symmetry and the sign of u^r, and assuming constant $z = 0$. A useful property is the "turning point", where u^r changes sign. This occurs at $u^r = 0$, with solution:

$$\frac{\ell}{e} = \frac{-g_{t\phi} \pm r}{g_{tt}} = r\frac{1 + \Omega r f v_s \mp \Omega r}{\Omega r + f v_s \mp 1}. \tag{19}$$

Figure 5 plots the turning points for the present spacetime parameters. In Minkowski spacetime or Newtonian physics, these would simply form a wedge $\ell/e = \pm r$, and correspond to the point of closest approach of a straight line to the origin. For the time machine with plateau f, this wedge graph does appear for $r \leq 1$ and $r \geq 4$. Also, we see from inspection that none of the outside null geodesics can reach the origin. The closest is for ℓ/e just above $5/6$, which reach to just beyond $r = 5/6$. There are two critical values of ℓ/e at $5/6$ and $\approx$3.85, where the minimum r attained by geodesics changes abruptly. This discontinuity is apparent in the diagram. Near the former value will turn out to be a rich parameter space for time travel. The latter corresponds to a turning point of Equation (19), which occurs at $r \approx 3.82$, with corresponding $\ell/e \approx 3.85$ as mentioned, which in turn has another intercept at $r \approx 2.70$.

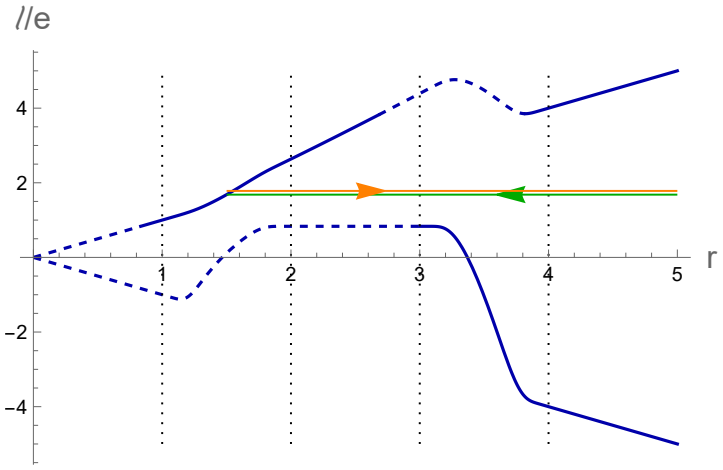

Figure 5. Turning points for null geodesics, where the blue plot satisfies $u^r = 0$ (Equation (19)). A sample trajectory is shown, which approaches inwards from large r. Since its impact parameter is constant, its worldline traces a horizontal line in the diagram. The first point of intersection with the blue curve corresponds to reaching its minimum r before traversing away, in general. The unbroken curves are the rightmost parts; only these are relevant to geodesics approaching from large r.

Figure 6 shows the amount of time travel for null geodesics. Similarly to before, we define this as the difference in the t coordinate between the entry and exit points on the boundary $r = 4$, plus a penalty of $r|\Delta\phi|$ for any angular offset, being the lab time (t) for a causal signal to return to the initial angle via a null circular arc. By definition, $\Delta t = 0$ for $\ell/e = \pm 4$ because these trajectories just graze the boundary.

Figure 7 exhibits the time travel to the past region by zooming in on Figure 6. From analytic and numerical investigation, it appears the number of loops increases without limit as $\ell/e \to 5/6$ from above, as does the time travel. In the figure, some points approach 1 μs of time travel. As before, having $\Delta t < 0$, as we have defined Δt, is a sufficient but not necessary condition for time travel because of our restricted choice of signal mechanism.

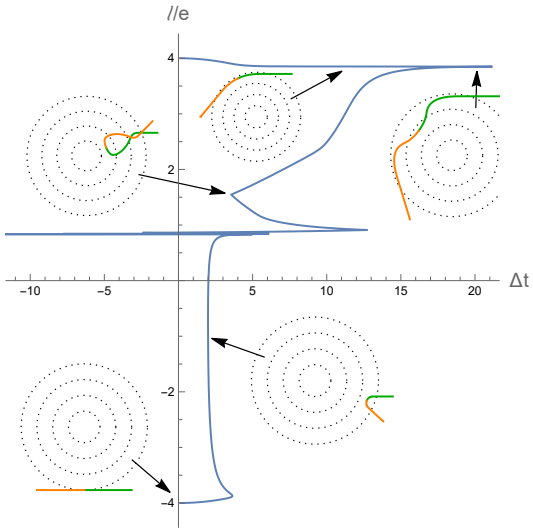

Figure 6. Total time travel for null paths in terms of impact parameter, with the same spacetime parameters $\Omega = 1.2$, $v_s = 1$, and plateau f. Some specific trajectories are shown as insets. Most of the parameter space has $\Delta t > 0$, meaning time travel is not achieved; however, see Figure 7 for the exceptions. The extended horizontal lines correspond to the critical values of ℓ/e discussed previously.

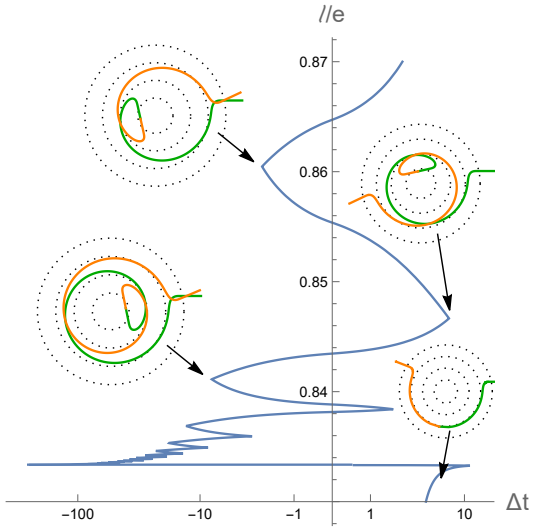

Figure 7. Time traveling null geodesics, a zoom in on Figure 6. In this region, the null curves make multiple loops, and most accrue substantial time travel—note the logarithmic scale. This reveals a sawtooth fractal pattern. The "teeth" on the left side are the local minima of Δt, that is, the local maxima of time travel. These correspond to paths which exit at the same ϕ as they entered, at least approximately. The teeth on the right are paths where the exit ϕ value is roughly opposite, which wastes signal travel time. The horizontal line is $\ell/e = 5/6$ or $0.8\bar{3}$.

6. Discussion

We have discovered and analyzed certain classes of geodesic trajectories in the Ralph and Chang time machine spacetime, which result in time travel. The time travel is a large-scale property of a trajectory. As we have defined it, it occurs relative to static observers in the flat spacetime region.We emphasize again, that the trajectories are locally future-pointing everywhere, and remain timelike or null.

Most geodesics are not time-traveling. Those which are most successful, which complete many loops inside the time machine region, can be very sensitive to parameters. On the other hand, we found some very generic choices of bubble functions f were sufficient, without any fine-tuning. For the case of the massive particle geodesics, it would be inter-

esting future work to look at the local environment (and tidal forces) of the particle as it traverses the trajectory. Another interesting future direction would be to try to engineer a collision between the ingoing and outgoing trajectories, thus forming an explicit geodesic CTC similar to the type discussed by Thorne et al. [3]. This would presumably require fine tuning of the parameters.

We also further analyzed the spacetime itself, obtaining a time orientation, and pointing out some Killing vector(s). We have also made a small contribution to the physical interpretation of spacetimes involving rotation, which has been a longstanding challenge in some cases. We also generalized Alcubierre's construction based on hypersurface–orthogonal observers to allow vorticity.

Author Contributions: Conceptualization; methodology; validation, C.M., F.C. and T.C.R.; writing—original draft preparation, C.M.; writing—review and editing, F.C. and T.C.R.; supervision, T.C.R. All authors have read and agreed to the published version of the manuscript.

Funding: This work was partially supported by the Australian Research Council Centre of Excellence for Quantum Computation and Communication Technology (Project No. CE110001027). Nordita is supported in part by NordForsk.

Data Availability Statement: No new data were created or analyzed in this study. Data sharing is not applicable to this article.

Conflicts of Interest: The authors declare no conflicts of interest.

Abbreviation

The following abbreviations are used in this manuscript:

CTCs closed timelike curves

Appendix A. Relative Velocity

Consider an observer $\mathbf{u}$, and a vector $\mathbf{n}$ at the same point in spacetime. The latter may be timelike, null, or spacelike. Recall velocity is displacement over time. In $\mathbf{u}$'s frame of reference, define the relative velocity of $\mathbf{n}$ as its space part divided by its time part, where this splitting is determined by $\mathbf{u}$. The pure time part of $\mathbf{n}$ is $-\langle \mathbf{n}, \mathbf{u} \rangle \mathbf{u}$ and pure space part: $\mathbf{n} + \langle \mathbf{n}, \mathbf{u} \rangle \mathbf{u}$, an orthogonal decomposition. The relative velocity $\vec{\mathbf{v}}$ follows from dividing these, where we use only the magnitude of the time part:

$$\vec{\mathbf{v}} = -\frac{1}{\langle \mathbf{n}, \mathbf{u} \rangle} \mathbf{n} - \mathbf{u}. \tag{A1}$$

Note that $\langle \mathbf{u}, \vec{\mathbf{v}} \rangle = 0$, so the relative velocity is purely spacelike according to $\mathbf{u}$ (or zero). Its length is the relative speed β, which is not limited by 1. Equation (A1) is invariant under the rescaling of $\mathbf{n}$. If $\mathbf{u}$ and $\mathbf{n}$ are orthogonal, then $\vec{\mathbf{v}}$ is not defined, and one might perhaps say the relative velocity is infinite, or more cautiously that $\mathbf{n}$ is purely spacelike according to our observer. Jantzen et al. [28], §2.1.4 give a similar result to Equation (A1), and also allow $\mathbf{n}$ to be timelike, null, or spacelike. Misner et al. [25], Equation (2.35), have essentially this formula for the special case of timelike $\mathbf{n}$.

Reversing the problem, we can rearrange it to obtain:

$$\mathbf{n} \propto \mathbf{u} + \vec{\mathbf{v}}. \tag{A2}$$

This shows how to construct a vector $\mathbf{n}$ with supplied relative velocity, subject to $\langle \mathbf{u}, \mathbf{u} \rangle = -1$ and $\langle \mathbf{u}, \vec{\mathbf{v}} \rangle = 0$. If the result is non-null, it may then be normalized. This generalizes the local Lorentz boost to the null and spacelike cases.

Appendix B. 4-Acceleration Formula

For a 4-velocity field $\mathbf{u}$, its 4-acceleration is $\mathbf{a} := \nabla_{\mathbf{u}}\mathbf{u}$, where ∇ is the Levi–Civita connection. The following is equivalent but computationally simpler [29], §7.8 and [28], §2.2.3:

$$\mathbf{a}^\flat = \mathbf{u} \lrcorner d\mathbf{u}^\flat. \tag{A3}$$

The flat symbol '$^\flat$' here denotes the covector corresponding to a vector, which in components is simply a_μ or u_μ. The notation '$\lrcorner$' is from differential forms, and means the vector $\mathbf{u}$ is substituted *into* the 2-form $d(\mathbf{u}^\flat)$. In a coordinate basis, we have simply $a_\nu = u^\mu(\partial_\mu u_\nu - \partial_\nu u_\mu)$. To show Equation (A3):

$$d\mathbf{u}^\flat \equiv \nabla\mathbf{u}^\flat - (\nabla\mathbf{u}^\flat)^T \tag{A4}$$

$$= -\mathbf{u}^\flat \wedge \mathbf{a}^\flat + 2\boldsymbol{\omega}, \tag{A5}$$

using the kinematic decomposition. The result follows. Here, '^{T}' is the transpose. We used the index-ordering convention $\nabla_\mu u_\nu$.

Appendix C. Generalized Warp Field Construction

Given any spacetime with metric, we "add" a warp field to obtain a new metric. This is based on Alcubierre's application of the lapse–shift formalism but generalized to a non-coordinate basis. This might be contrasted with the Kerr–Schild ansatz or Gordon form. Suppose a 4-velocity field $\mathbf{u}$ is provided, along with some "warp shift" 4-vector field $\mathbf{b}$ satisfying $\langle \mathbf{u}, \mathbf{b} \rangle = 0$, and "warp lapse" α. The specific values used for the Alcubierre and time machine spacetimes are given in Sections 2.1 and 2.3. Whereas the standard lapse–shift construction takes 3-dimensional metrics on hypersurfaces and welds them into a 4-dimensional metric, we take one 4-dimensional metric and define a new one:

$${}^{\text{warp}}g_{\mu\nu} := \big(1 - \alpha^2 + \langle \mathbf{b}, \mathbf{b} \rangle\big) u_\mu u_\nu - u_\mu b_\nu - b_\mu u_\nu + {}^{\text{original}}g_{\mu\nu} \tag{A6}$$

Note that in Equation (A6) (and throughout this Appendix), all angle brackets and the raising or lowering of indices refer to the original metric, ${}^{\text{original}}g_{\mu\nu}$. By design, the metric components match the standard lapse–shift metric [25], §21.4, when expressed in an adapted basis $(\mathbf{u}, \mathbf{e}_1, \ldots)$. (The $\mathbf{e}_i$ satisfy $\langle \mathbf{u}, \mathbf{e}_i \rangle = 0$, but need not be constructed.) The extra '1' appears because the spatial metric is $\mathbf{u}^\flat \otimes \mathbf{u}^\flat + ds^2_{\text{original}}$. The dual co-basis is $(-\mathbf{u}^\flat, \mathbf{e}^1, \ldots)$. The analogue of the Eulerian observers is $(\mathbf{u} - \mathbf{b})/\alpha$, which is dual to $\alpha\mathbf{u}^\flat$ under the *new* metric, and normalized. We label it the warp velocity (c.f. Section 3).

What happens to the original observers $\mathbf{u}$ after the warp field is added, for example, the platform? Physically, it seems questionable to claim a correspondence between vectors in different spacetime regions. Hence, we *define* those observers to have relative velocity $\mathbf{b}/\alpha$ in the warp frame. Note that this is orthogonal to the warp velocity in the new metric. Hence, add them to obtain $\mathbf{u}/\alpha$ (see Equation (A2)). This vector has squared-norm $\langle \mathbf{b}, \mathbf{b} \rangle/\alpha^2 - 1$, so it is not necessarily timelike. (This expression uses the warp metric, despite being expressed in terms of the original metric.) The relative speed is $\sqrt{\langle \mathbf{b}, \mathbf{b} \rangle}/\alpha$, which is possibly superluminal.

Notes

[1] Intuitively, the bubble is a topological ball, at least under the original Minkowski metric as restricted to a hypersurface $t = \text{const}$. Alcubierre's f only approaches 0 asymptotically, and hence is not compactly supported, but one might consider instead $f \geq \tilde{\epsilon}$ for some small constant.

[2] For the special case $g_{\phi\phi} = 0$, we have instead:

$$u_\mu = \Big(\ell \frac{g_{tt}}{2g_{t\phi}} + \frac{\epsilon g_{t\phi}}{2\ell}, 0, \ell, 0\Big).$$

Note that for $g_{\phi\phi} = 0$, both g_{tt} and $g_{t\phi}$ must be nonzero for a nondegenerate metric, and $\ell \neq 0$ for any nonzero vector.

References

1. Gödel, K. An Example of a New Type of Cosmological Solutions of Einstein's Field Equations of Gravitation. *Rev. Mod. Phys.* **1949**, *21*, 447–450. [CrossRef]
2. Ellis, G.F.R. Editor's Note. *Gen. Relativ. Gravit.* **2000**, *32*, 1399–1408. [CrossRef]
3. Echeverria, F.; Klinkhammer, G.; Thorne, K.S. Billiard balls in wormhole spacetimes with closed timelike curves: Classical theory. *Phys. Rev. D* **1991**, *44*, 1077–1099. [CrossRef] [PubMed]
4. Friedman, J.; Morris, M.S.; Novikov, I.D.; Echeverria, F.; Klinkhammer, G.; Thorne, K.S.; Yurtsever, U. Cauchy problem in spacetimes with closed timelike curves. *Phys. Rev. D* **1990**, *42*, 1915–1930. [CrossRef] [PubMed]
5. Hawking, S.W. Chronology protection conjecture. *Phys. Rev. D* **1992**, *46*, 603–611. [CrossRef] [PubMed]
6. Krasnikov, S. Time machines with the compactly determined Cauchy horizon. *Phys. Rev. D* **2014**, *90*, 024067. [CrossRef]
7. Deutsch, D. Quantum mechanics near closed timelike lines. *Phys. Rev. D* **1991**, *44*, 3197–3217. [CrossRef] [PubMed]
8. Politzer, H.D. Path integrals, density matrices, and information flow with closed timelike curves. *Phys. Rev. D* **1994**, *49*, 3981–3989. [CrossRef] [PubMed]
9. Lloyd, S.; Maccone, L.; Garcia-Patron, R.; Giovannetti, V.; Shikano, Y.; Pirandola, S.; Rozema, L.A.; Darabi, A.; Soudagar, Y.; Shalm, L.K.; et al. Closed Timelike Curves via Postselection: Theory and Experimental Test of Consistency. *Phys. Rev. Lett.* **2011**, *106*, 040403. [CrossRef] [PubMed]
10. Visser, M. The Kerr spacetime: A brief introduction. *arXiv* **2007**, arXiv:0706.0622.
11. Tippett, B.K.; Tsang, D. Traversable acausal retrograde domains in spacetime. *Class. Quantum Gravity* **2017**, *34*, 095006. [CrossRef]
12. Ori, A. A Class of Time-Machine Solutions with a Compact Vacuum Core. *Phys. Rev. Lett.* **2005**, *95*, 021101. [CrossRef]
13. Ori, A. Formation of closed timelike curves in a composite vacuum/dust asymptotically flat spacetime. *Phys. Rev. D* **2007**, *76*, 044002. [CrossRef]
14. Soen, Y.; Ori, A. Improved time-machine model. *Phys. Rev. D* **1996**, *54*, 4858–4861. [CrossRef]
15. Mallary, C.; Khanna, G.; Price, R.H. Closed timelike curves and 'effective' superluminal travel with naked line singularities. *Class. Quantum Gravity* **2018**, *35*, 175020. [CrossRef]
16. Alcubierre, M. Letter to the editor: The warp drive: Hyper-fast travel within general relativity. *Class. Quantum Gravity* **1994**, *11*, L73–L77. [CrossRef]
17. Krasnikov, S.V. Hyperfast travel in general relativity. *Phys. Rev. D* **1998**, *57*, 4760–4766. [CrossRef]
18. Olum, K.D. Superluminal Travel Requires Negative Energies. *Phys. Rev. Lett.* **1998**, *81*, 3567–3570. [CrossRef]
19. Natário, J. Warp drive with zero expansion. *Class. Quantum Gravity* **2002**, *19*, 1157–1165. [CrossRef]
20. Bobrick, A.; Martire, G. Introducing physical warp drives. *Class. Quantum Gravity* **2021**, *38*, 105009. [CrossRef]
21. Everett, A.E. Warp drive and causality. *Phys. Rev. D* **1996**, *53*, 7365. [CrossRef] [PubMed]
22. Ralph, T.C.; Chang, C. Spinning up a time machine. *Phys. Rev. D* **2020**, *102*, 124013. [CrossRef]
23. Lobo, F.S.N.; Visser, M. Fundamental limitations on 'warp drive' spacetimes. *Class. Quantum Gravity* **2004**, *21*, 5871–5892. [CrossRef]
24. Fermi, D.; Pizzocchero, L. A time machine for free fall into the past. *Class. Quantum Gravity* **2018**, *35*, 165003. [CrossRef]
25. Misner, C.; Thorne, K.; Wheeler, J. *Gravitation*; W.H. Freeman and Co.: New York, NY, USA, 1973.
26. Gourgoulhon, E. *3+1 Formalism in General Relativity*; Springer: Berlin/Heidelberg, Germany, 2012; Volume 846. [CrossRef]
27. Alcubierre, M.; Lobo, F.S.N. Warp Drive Basics. *Fundam. Theor. Phys.* **2017**, *189*, 257. [CrossRef].
28. Jantzen, R.; Carini, P.; Bini, D. *GEM: The User Manual: Understanding Spacetime Splittings and Their Relationships*; Unpublished work, 2013.
29. Hestenes, D.; Sobczyk, G. *Clifford Algebra to Geometric Calculus*; Springer: Berlin/Heidelberg, Germany, 1984.